Naval Research Laboratory

Washington, DC 20375-5000

NRL Memorandum Report 5990

Integrity Analysis of a T-Frame Stiffened Panel with a Weld Defect

V. GENSHEIMER DEGIORGI AND P. MATIC

Mechanics of Materials Branch
Materials Science and Technology Division

J. JUDY

David Taylor Research Center
Bethesda, MD 20084-5000

M. I. JOLLES

Mechanics of Materials Branch
Materials Science and Technology Division

December 9, 1988

SECURITY CLASSIFICATION OF THIS PAGE

ADA204977

REPORT DOCUMENTATION PAGE

Form Approved
OMB No. 0704-0188

1a. REPORT SECURITY CLASSIFICATION UNCLASSIFIED	1b. RESTRICTIVE MARKINGS
2a. SECURITY CLASSIFICATION AUTHORITY	3. DISTRIBUTION / AVAILABILITY OF REPORT Approved for public release; distribution unlimited.
2b. DECLASSIFICATION / DOWNGRADING SCHEDULE	
4. PERFORMING ORGANIZATION REPORT NUMBER(S) NRL Memorandum Report 5990	5. MONITORING ORGANIZATION REPORT NUMBER(S)
6a. NAME OF PERFORMING ORGANIZATION Naval Research Laboratory 6b. OFFICE SYMBOL (If applicable) Code 6382	7a. NAME OF MONITORING ORGANIZATION
6c. ADDRESS (City, State, and ZIP Code) Washington, D.C. 20375-5000	7b. ADDRESS (City, State, and ZIP Code)
8a. NAME OF FUNDING / SPONSORING ORGANIZATION Office of Naval Research 8b. OFFICE SYMBOL (If applicable)	9. PROCUREMENT INSTRUMENT IDENTIFICATION NUMBER
8c. ADDRESS (City, State, and ZIP Code) Arlington, VA 22217	10. SOURCE OF FUNDING NUMBERS PROGRAM ELEMENT NO: 61153N PROJECT NO: RR022-01-48 TASK NO: WORK UNIT ACCESSION NO: DN080-024

11. TITLE (Include Security Classification)

Integrity Analysis of a T-Frame Stiffened Panel with a Weld Defect

12. PERSONAL AUTHOR(S)

DeGiorgi, V.G., Matic, P., Judy,* J. and Jolles, M.I.

13a. TYPE OF REPORT	13b. TIME COVERED	14. DATE OF REPORT (Year, Month, Day)	15. PAGE COUNT
	FROM _____ TO _____	1988 December 9	27

16. SUPPLEMENTARY NOTATION

*David Taylor Research Center, Bethesda, MD 20084-5000

17. COSATI CODES		
FIELD	GROUP	SUB-GROUP

18. SUBJECT TERMS (Continue on reverse if necessary and identify by block number)

Integrity analysis, Strain energy
Weld
Fracture
Finite element

19. ABSTRACT (Continue on reverse if necessary and identify by block number)

Structural integrity analyses are often an essential part of the design and fabrication processes. In any structural integrity analysis, an accurate representation of component geometry and material constitutive response is required. Weld geometry and weld inhomogenity add to the complexity of a structural integrity analysis. The current work consist of a structural integrity analysis of a welded T-frame stiffened panel with a lack of penetration weld defect. Material fracture toughness at the continuum scale is used in the computational simulation of the welded T-frame. Complementary global and detial weld defect region models are used to simulate global and local structural response. Differences in weld and base metal properties are explicitly included in the computational simulation. The failure site is determined directly from the computational analysis.

20. DISTRIBUTION / AVAILABILITY OF ABSTRACT ☒ UNCLASSIFIED/UNLIMITED ☐ SAME AS RPT ☐ DTIC USERS	21. ABSTRACT SECURITY CLASSIFICATION UNCLASSIFIED
22a. NAME OF RESPONSIBLE INDIVIDUAL Virginia Gensheimer DeGiorgi	22b. TELEPHONE (Include Area Code) (202) 767-9027 22c. OFFICE SYMBOL Code 6382

DD Form 1473, JUN 86 Previous editions are obsolete SECURITY CLASSIFICATION OF THIS PAGE

S/N 0102-LF-014-6603

CONTENTS

INTEGRITY ANALYSIS OF A T-FRAME STIFFENED PANEL WITH A WELD DEFECT

INTRODUCTION

Welded joints are an essential part of many structural systems. Defects due to lack of penetration and inclusion of slag can exist as artifacts of the welding process. The potentially detrimental effects of defects on the load carrying capability of structures makes the presence of defects of concern to the designer and structural analyst.

The presence of defects in a weld can be determined by non-destructive test techniques such as ultrasonic and radiographic examination. If the presence of a defect has been established it is essential to determine if the defect is detrimental to the structure. Arbitrary limits on defect dimensions tend to be based on workmanship quality rather than detailed analytical evaluation of weld strength [1]. Investigations, such as those performed by Sandor [2] and Boulton [3], have been conducted in an attempt to quantify the process of determining an acceptable defect size. Detailed analytical structural integrity evaluation of a weld containing a defect could indicate acceptance of a defect larger than the arbitrary workmanship based limits therefore eliminating weld performance degradation which may occur as a result of the repair process [1].

One approach to the structural integrity evaluation of a welded joint with a known defect is to assume that the defect is the most severe type possible. The resulting evaluation is a fracture mechanics analysis of a crack like defect. Linear elastic fracture theories have been used to successfully predict brittle fracture. However, brittle fracture is only one of many possible structural failure mechanisms[4]. High toughness materials may exhibit large amounts of local deformation prior to fracture. In order to accurately predict failure in high toughness materials, damage and fracture theories which address ductile behavior are required.

Many failure criteria have been proposed for ductile materials. Predominant among the failure criteria proposed are contour integrals such as J [5] and crack tip opening displacement [6]. Some early work in the determination of ductile failure criteria used correction factors to extend the region of applicability of linear elastic fracture mechanics by representing the effects of plasticity around the crack tip [7,8]. However, only a limited amount of plasticity can be accounted for by correction factors.

Manuscript approved October 5, 1988.

In general, when there is a relatively small amount of plasticity around the crack tip, failure criteria based on linear elastic concepts can be used successfully. However, in instances where large amounts of plasticity occur prior to failure, analysis methods based on linear elastic concepts are no longer capable of approximating the state of stress and strain near the crack tip. In order to accurately represent the state of stress and strain near the crack tip the analysis method and failure criteria used should explicitly include large deformation constitutive response.

The explicit consideration of ductile material behavior prior to fracture does not in and of itself alleviate all limitations which may be associated with a particular fracture mechanics analysis technique. Present day fracture mechanics analysis techniques have limitations which must be taken into consideration [9]. Limitations common to fracture mechanics analysis techniques include the mathematical prediction of physically unattainable conditions such as the existence of a stress, strain and strain energy density singularity, correct material characterization and the appropriateness of the chosen fracture criterion. The material characterization used for ductile fracture should include an accurate description of large strain response. The failure criterion for ductile fracture should not be limited by the amount of local deformation which occurs prior to fracture. Other areas of concern which may exits for specific problems include availability of suitable data to adequately characterize material deformation, effects of loading rate and history, interpretations of material data scatter and defect characterization.

In addition to the various limitations listed above, a feature common to many fracture criteria is the assumption that failure occurs at a dominant crack or defect which is observed or assumed to exist in the structure. Since failure is assumed to occur at a crack or a defect, these features must be present in the test specimen used to determine the critical values of the parameters in the fracture criterion.

A material damage and failure criterion which explicitly addresses ductile behavior can be developed based on a general continuum approach which utilizes the constitutive relations to describe deformation, damage and fracture by the continuous point variables of stress, strain and energy density. Continuum material toughness [10] is one such material damage and fracture criterion. For a structural analysis, the geometry and boundary conditions

which define the problem and the constitutive relations representing the material are used in a computational solution for the stress, strain and energy density fields. The critical locations in the structure are identified from the computational simulation and the load or time to failure is determined from the local stress, strain and energy density histories. A priori assumptions regarding the location and mode of failure are not required. The failure criterion used is the strain energy density required to produce material fracture at the continuum scale. The use of an energy density as a failure criterion is consistent with the concepts presented by Freudenthal [11] on material behavior and scaling considerations. Previous work by Gillemot [12] used analytical and empirical techniques to determine the strain energy density per unit volume at fracture for cylindrical tensile specimens. The strain energy per unit volume absorbed by the material up to the instant of fracture was calculated from global specimen load-displacement response and deformed geometry. A computational simulation of a welded T-section using the strain energy density at the continuum scale as the failure criterion was performed by Matic and Jolles [13]. The critical strain energy density was determined from continuum stress-strain information obtained from tensile tests and percent reduction in area in a manner similar to that detailed in the current work. The failure load obtained from a nonlinear finite element analysis compared favorably with the failure load obtained from a laboratory test of the T-section performed subsequent to the numerical prediction.

In the current work strain energy density concepts and analysis procedures are reviewed and applied in a structural integrity analysis of a welded T-frame stiffened panel. The fracture initiation load and location of failure are determined from a finite element simulation.

CONTINUUM MATERIAL TOUGHNESS CONCEPTS

A continuum volume of material undergoing deformation is characterized by its multiaxial stress and strain state, σ_{ij} and ε_{ij}, respectively. For ductile metals, and other materials which exhibit inelastic deformation, the strain state is a function of the stress history as well as the stress state. The state of stress and strain may be related by a constitutive formulation which defines the strain increment $\Delta\varepsilon_{ij}$ from the current stress state.

The strain energy per unit mass at a given instant during deformation is:

$$w = \lim_{\Delta V \to 0} \frac{\rho \Delta W}{\Delta V} \tag{1}$$

$$= \int_0^{\varepsilon_{ij}} \frac{\sigma_{ij} d\varepsilon_{ij}}{\rho} \tag{2}$$

where ρ is the mass density. The energy density incorporates both stress and strain into a fundamental quantity relevant to thermodynamic description of material deformation and damage. The energy density is a scalar quantity which takes into account all components of the stress and strain tensors in a physically consistent manner. Failure of the material, at the continuum scale, can be associated with the value of the energy density at which fracture occurs. Thus, the material toughness may be defined as:

$$w_c = \int_0^{(\varepsilon_{ij})_c} \frac{\sigma_{ij} d\varepsilon_{ij}}{\rho} \tag{3}$$

where w_c is the critical strain energy density. The value of w_c can be considered as a material property for structural analyses.

For ductile materials, the material density varies only slightly, even over large deformations. For this reason, it is possible to define an energy per unit volume density as:

$$w = \lim_{\Delta V \to 0} \frac{\Delta W}{\Delta V} \tag{4}$$

$$= \int_0^{\varepsilon_{ij}} \sigma_{ij} d\varepsilon_{ij} \tag{5}$$

with an associated critical value

$$w_c = \int_0^{(\varepsilon_{ij})} \sigma_{ij} d\varepsilon_{ij} \tag{6}$$

The energy per unit mass is fundamental, however the energy per unit volume is equally appropriate for constant volume deformation processes.

For the case of an uniaxial stress-strain curve, corresponding to a one-dimensional state of deformation, the critical strain energy density corresponds to the area under the uniaxial stress-strain curve:

$$w_c = \int_0^{\varepsilon_c} \sigma d\varepsilon \tag{7}$$

This representation is desirable for use with traditional constitutive formulations which rely on equivalent uniaxial stress-strain curves. In the general case of multiaxial stress and strain, the strain energy density is the sum of the integrals of the individual stress and strain components.

A structural integrity analysis should identify the location of fracture initiation as well as the magnitude of the failure load. A priori selection of the fracture initiation site should not be necessary. In multi-material structures, a relative strain energy density ratio may be used to determine the location of failure and to establish the relative tendency for fracture in each constituent material. The relative strain energy density is the ratio of the local strain energy density attained in the loading process divided by the appropriate local critical strain energy density:

$$\left[\frac{w}{w_c}\right]_n < 1.0 \qquad n=1, 2, 3, \ldots, N \tag{8}$$

where N is the total number of materials in the structure. When values of this ratio are less than unity, fracture initiation does not occur. When the relative strain energy density ratio reaches unity at a site in one of the constituent material, represented by n_c, so that

$$\left[\frac{w}{w_c}\right]_{n_c}=1.0 \tag{9}$$

and

$$\left[\frac{w}{w_c}\right]_n < 1.0 \qquad n=1, \ldots, n_c-1, n_c+1, \ldots, N \tag{10}$$

fracture occurs in material n_c.

T-FRAME STIFFENED PANEL GEOMETRY

The present analysis evaluates the structural integrity of a T-frame stiffened panel with a defect in the weld. The section dimensions are as shown in Figure 1. The panel is 96.0 inches long and 0.375 inches thick. The stiffener web and flange are 0.200 inches thick. The web is 10.0 inches deep and the flange is 4.0 inches wide. Both ends of the panel are rigidly connected to the remaining structure. Multiple panel spans are connected for fabrication the parent structure. The distance between stiffeners is 27.0 inches. The panel is subjected to an external pressure load as shown in Figure 1. The T-frame panel and associated loading are typical of the type of component and applied load which may be found in large welded structures. The T-frame stiffened panel is made of HT structural steel and the weld is made of short arc weld material.

The T-frame stiffener is made of two stiffeners welded together at the span centerline. A lack of penetration defect is included in the computational simulation model in the stiffener flange at the weld centerline. The defect has an cross section as shown in Figure 2 and extends for half the stiffener thickness.. The defect spans the entire width of the panel. A defect of this type and size is detectable by non-destructive examination techniques [14].

MATERIAL CHARACTERIZATION

Data from flat welded tensile specimens was available to characterize base metal and weld metal material behavior. The specimens were 0.2 inches thick base metal plates which had been welded together. The welded plates were cut into flat tensile specimens with the weldline spanning the specimen width.

The specimens fractured in either the base metal adjacent to the weld metal or in the weld metal itself. No explicit treatment of

the heat affected zone was made due to the tensile specimen size and geometry. The occurrences of fracture in the base metal adjacent to the weld included the effects of the heat affected zone, in an average sense, in the base metal characterization. Standard Cauchy stress-logarithmic strain curves were developed from specimen load displacement data. The stress-strain curves exhibited significant scatter but no distinguishing trend differentiating base metal failure and weld metal failure specimens (Figure 3). The percent reduction in area (%RA), however, while also exhibiting scatter, clearly divided the failed specimens into two distinct groups. The base metal failures fell into the range of 33.0 - 67.0 %RA while the weld metal failures fell into the range of 0.5 - 6.3 %RA.

The marked difference between base metal and weld metal ductility is not apparent from uniaxial considerations alone. Accurate evaluation of the different material toughnesses requires accurate equivalent Cauchy stress-logarithmic strain representations. Such representations should quantitatively reflect the material ductility present in three-dimensional states of deformation. In order to accomplish this quantitative representation continuum stress-strain curves for the base metal and the weld metal (Figure 4) were generated using a procedure previously applied to ductile materials [15]. The procedure is based on results which indicate that the actual continuum stress-strain curves will be more nonlinear than either the standard Cauchy stress-logarithmic strain curve determined from data spanning the entire range of deformation or stress-strain curves extrapolated from small strain data. Subsequent to the work presented in this paper, refinements of the procedure have been reported [16,17].

The critical strain energy density of the base metal at fracture was calculated based on the average base metal %RA. Average base metal %RA was used since the base metal was essentially defect free and the %RA is influenced by weld geometry, which may be either detrimental or beneficial to the apparent base metal toughness. The base metal critical strain energy density determined from the continuum stress-strain curves and the average %RA is 54,023 psi.

The critical strain energy density of the weld metal was calculated based on the maximum weld metal %RA. The maximum %RA was used since the presence of lack of penetration defects in the weld metal will tend to degrade the strength of the weld metal resulting in an reduction in the apparent toughness in a manner

similar to the reduction in weldment fatigue strength caused by the presence of defects [18]. The maximum %RA is the limiting case which minimizes the influence of defects in the weld metal failure specimen and provides a lower bound on the weld metal material toughness. The critical strain energy density for the weld metal determined from the continuum stress-strain curves and the maximum %RA is 4087 psi.

FINITE ELEMENT ANALYSIS

Dimensional variation in structural features often introduce an additional level of complexity to integrity analyses. In many welded structures the weld is a small fraction of the entire structure and any defects are usually only a fraction of the weld size. It is possible for many orders of magnitude to exist between the component and defect dimensions. The numerical evaluation of the welded structure must take into account this range of dimensions. One way to include both the overall geometry and the defect geometry is to create one finite element model of the entire structure which is refined enough to capture the stress and strain profile near the defect. This approach results in extremely large models which tax both the computer and financial resources available to the analyst.

A more reasonable approach, both with respect to model size and analysis cost, requires global and local regional models. The global response of the structure is determined from a finite element model of the component. No flaw is included in the global response model so that element size is based on gross structural feature dimensions. The local stress, strain and strain energy response in the vicinity of the defect is obtained from a second more refined model. The refined model includes the defect and the element size is based on the defect dimensions. The models are designed so that complimentary information is obtained from each analysis.

The complete structural response is obtained by combining results from the global and local analyses as shown in Figure 5.

Global Response Analysis

The global response of the T-frame stiffened panel is determined from a static nonlinear ABAQUS [19] finite element analysis. The global model is shown in Figure 6 and consists of 156

type S8R shell elements. These are 8-noded generalized shell elements with variable thickness capabilities. The generalized shell element used in ABAQUS is based on a standard three-dimensional isoparametric continuum element [20]. The three-dimensional element is compressed in the thickness direction through manipulation of the displacement interpolation scheme. Penalty functions are used along with displacement interpolation in such a manner so that the resulting strain through the thickness is zero. This modified element can be used to model thin shell behavior.

Load and T-frame geometry symmetry allow for use of a half length model. The panel section of the finite element model is extended to half the distance between longitudinally connected T-frames. The ends of the span are assumed to be rigidly fixed. The finite element model is subjected to a uniform pressure against the outer panel surface.

The global response finite element model is designed to obtain the response of a defect free T-frame stiffened panel. The entire model is assigned base metal continuum stress-strain material properties since the shell elements are significantly larger than the weld metal region. The bulk response of the panel is not affected by the absence of weld metal in the finite element simulation.

Geometric and material nonlinearities are included in the finite element simulation. Geometric nonlinearity is included to account for large strains and rotations which may occur locally prior to failure. A modified Rik's algorithm is used in the solution to assure numerical stability independent of structural stability. Increments of load are based on increments of path length along the load-displacement solution which result in convergent numerical solutions. In the modified Rik's algorithm the magnitude of the applied load is an unknown to be determined as part of the solution.

Defect Region Analysis

In order to obtain the local stress, strain and strain energy density behavior near the defect, a three-dimensional continuum element model was created of the region surrounding the defect. The defect region model consists of a portion of the stiffener flange and web. Both the flange and web are extended a sufficient distance to allow for local stress and strain attenuation. The weld crown is

included in the defect region model. A static nonlinear finite element analysis is performed using the computer code ABAQUS [19].

The three-dimensional model of the defect region (Figure 7) consists of 518 C3D20 and C3D20H elements. These are 20-noded continuum elements with quadratic displacement interpolation. In edition to displacement interpolation, the C3D20H elements incorporate an independently interpolated linear hydrostatic stress component [20]. LaGrange multipliers are used to couple the hydrostatic stress component to the constitutive relationship. The use of such hybrid elements in regions of larger deformation in the model, such as near the defect, prevent physically unrealistic displacement constraints from propagating through the mesh. These unrealistic displacement constraints artificially increase the model stiffness for incompressible or nearly incompressible material deformations.

Geometric and material nonlinearities are included in the defect region finite element evaluation. As in the global response analysis, a modified Rik's algorithm is used to assure solution stability.

The defect region model consists of two materials. Material properties are based on the continuum stress-strain response and %RA as described in Section III. The weld crown and a section of the flange extending from the weld crown are assigned weld metal material properties as shown in Figure 4. The remainder of the model is assigned base metal material properties. No heat affected zone is included in the model.

It is not possible for the external pressure loading to be directly applied to the defect region model. The external pressure is applied to the defect region model by imposing the displacements from the global response analysis onto the edge elements of the defect region model. In the current analysis component failure is defined as fracture initiation. Fracture initiation occurs when the strain energy density reaches the local material toughness value. The location of failure is determined from the defect region finite element analysis.

Discussion of Results

The global response of the T-frame stiffened panel is obtained from the ABAQUS shell model. The maximum longitudinal displacement on the outer surface of the stiffener flange occurs at the span centerline. The global applied load-maximum longitudinal displacement curve is shown in Figure 8.

The defect region model is used to determine the location of failure with the T-frame stiffened panel. The variation in strain energy density in the vicinity of the defect with increasing external pressure is shown in Figure 9. Failure by fracture initiation occurs when the critical strain energy density is reached at a point immediately above the defect at the web centerline at a maximum panel displacement of 0.027 inches. The global response finite element analysis results correlate a panel displacement of 0.027 inches with an external pressure of 84.0 psi.

CONCLUSIONS

Material toughness at the continuum scale may be appropriately defined using the critical strain energy per unit mass at fracture. The critical value of the strain energy density can be determined from appropriate interpretation of information obtained from simple material tests, such as the tensile test. For uniaxial material test geometries, the standard Cauchy stress-logarithmic strain curve developed from specimen load-displacement response is not an accurate description of the material constitutive response for large deformations which may occur prior to fracture in ductile materials. A more accurate continuum stress-strain curve can be developed from uniaxial test data and the percent reduction in area.

The current analysis demonstrates use of material toughness at the continuum scale as the failure criterion in a multi-material structural analysis. The computational analysis performed does not incorporate a priori assumptions of the location or mode of failure. The continuum basis of the critical strain energy density as a fracture criterion eliminates any need to assume the location of failure.

In the present analysis a T-frame stiffened panel is shown to be sensitive to a lack of penetration weld defect. The strain energy density required for fracture at the continuum scale is used as the failure criterion. Two nonlinear finite element analyses using the computer code ABAQUS were performed as part of the structural integrity analysis. A simple, relatively coarse finite element model was used to obtain the global component behavior. A detailed three-dimensional finite element model of the region containing the defect was used to obtain the local stress, strain and strain energy fields.

ACKNOWLEDGEMENTS

The authors wish to acknowledge the interest and support of Messrs. Peter M. Palermo and J. Allan Manuel of the Naval Sea Systems Command.

REFERENCES

1. Harrison, J. D., "The Economics of a Fitness for Purpose Approach to Weld Defect Acceptance," Fitness for Purpose Validation of Welded Constructions, P45.1-P45.10 (1982).

2. Sandor, L. W., "The Significance of Weld Discontinuities in Ship Hulls," U. S. Dept. of Commerce, 3-36233 Task S-22 (1980).

3. Boulton, C. F., "Fatigue Life Predictions of Welded Specimens Containing Lack of Penetration Defects at Ambient and Elevated Temperatures," Int. J. Pressure Vessel and Piping, Vol. 4, 171-195 (1976).

4. ASTM Metals Handbook, Vol. 10, Failure Analysis, ASTM (1978).

5. Rice, J. R., "A Path Independent Integral and the Approximate Analysis of Strain Concentration by Notches and Cracks," J. of Applied Mechanics, Vol. 35, 379-386 (1968).

6. Wells, A. A., "Applications of Fracture Mechanics At and Beyond General Yield," British Welding Res. Assc. Rpt., M13/63 (1963).

7. Dugdale, D. S., "Yielding of Steel Sheets Containing Slits," J. of Mechanics of Physics and Solids, Vol. 8, 100-108 (1960).

8. Hahn, G., T., Sarrate, M., and Rosenfeld, A. R., "Criteria for Crack Extension in Cylindrical Pressure Vessels," Int. J. of Fracture, Vol. 5, 187-210 (1969).

9. Clark, W. G., Jr., "Some Problems in the Applications of Fracture Mechanics," Fracture Mechanics - 13th Conference, ASTM STP 743, 269-287 (1981).

10. Matic, P. and Jolles, M. I., "Fracture Mechanics, Strain Energy Density and Critical Issues for Research and Applications," NRL Memo. Rpt. 6583 (1986).

11. Freudenthal, A. M., The Inelastic Behavior of Engineering Materials and Structures (1950).

12. Gillemot, L. F., "Criterion of Crack Initiation and Spreading," Engineering Fracture Mechanics, Vol. 8, 239-253 (1976).

13. Matic, P. and Jolles, M. I., "Defects, Constitutive Behavior and Continuum Toughness Considerations for Weld Integrity Analysis," NRL Memo. Rpt. 5935 (1987)

14. Boothroyd, C. A. and Garrett, G. C., "Ultrasonic Detection Variability of Weld Defects and the Effects on Fracture Mechanics Predictions - An Experimental Assessment," FWP Journal, Vol. 24, No. 7, 19-40 (1984).

15. Matic, P., "Numerically Predicting Ductile Material Behavior from Tensile Specimen Response," Theoretical and Applied Fracture Mechanics, Vol. 4, 13-28 (1985).

16. Matic, P., Kirby, G. C. III, and Jolles, M. I., "The Relationship of Tensile Size and Geometry Effects to Unique Constitutive Parameters for Ductile Materials," NRL Memo. Rpt. 5936 (1987).

17. Matic, P., Kirby, G. C. III, Father, P. and Jolles, M. I., "Determination of Ductile Alloy Constitutive Response by Iterative Finite Element and Laboratory Video Image Correlation," NRL Memo. Rpt. 6233 (1988).

18. Balasubramaniam, S., and Prasannakumar, S., "Defect Tolerance of Steel Weldments," Indian Welding Journal, April, 58-68 (1982).

19. Hibbitt, H. D., Karlsson, B. I. and Sorensen, E. P., ABAQUS User's Manual (1984).

20. Hibbitt, H. D., Karlsson, B. I. and Sorensen, E. P., ABAQUS Theory Manual (1984).

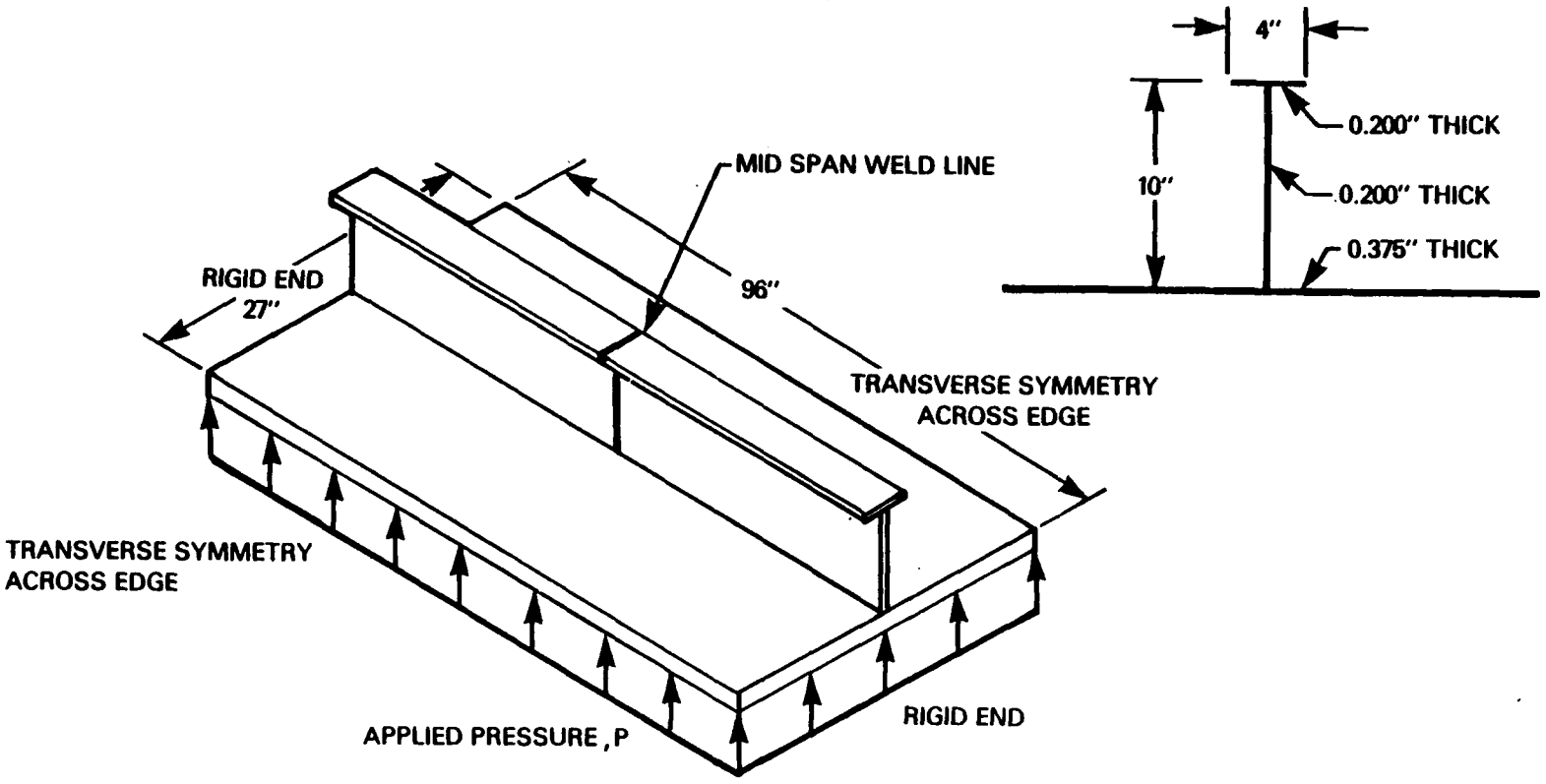

FIGURE 1: T-Stiffened Panel Geometry

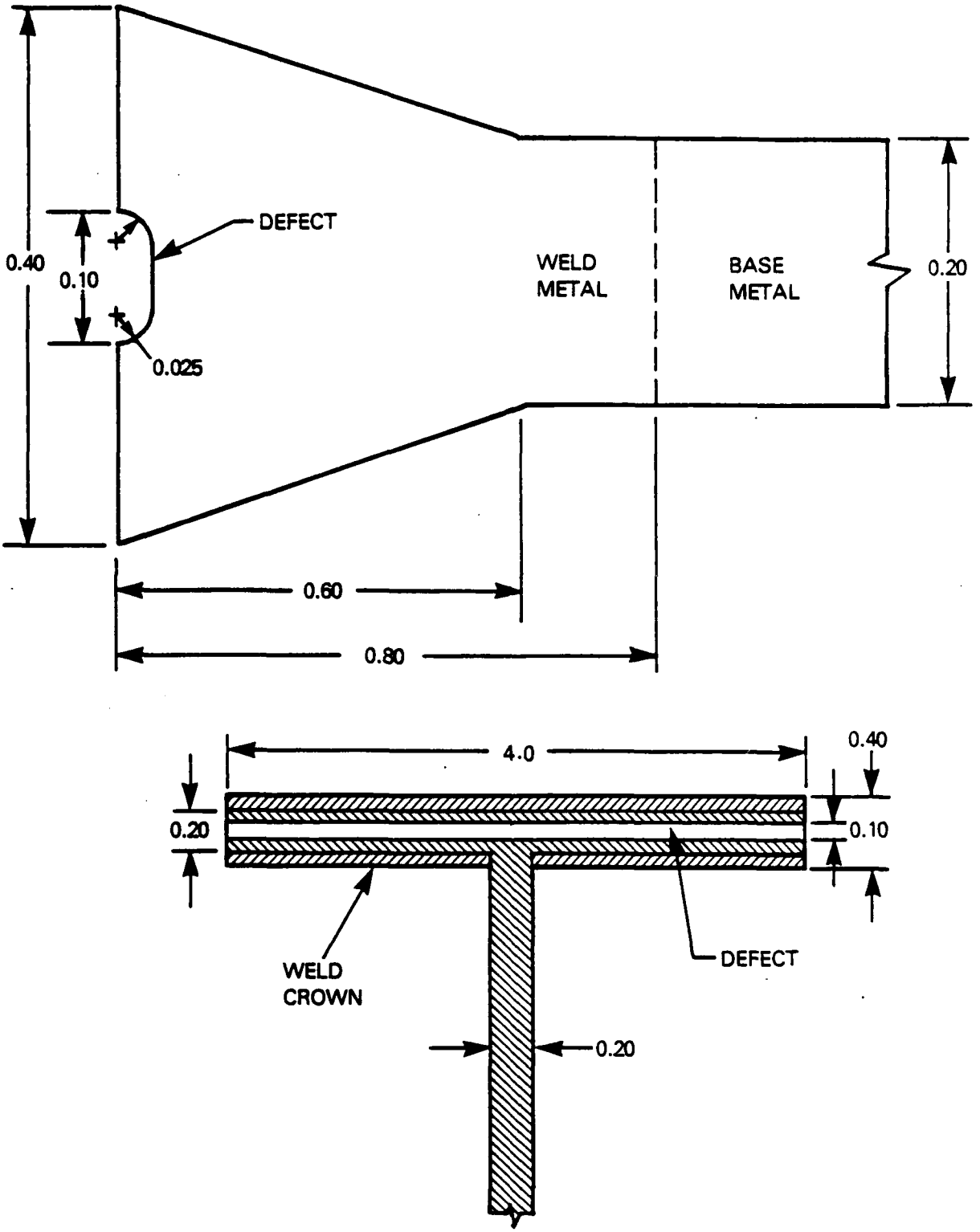

FIGURE 2: Lack of Penetration Defect included in T-Frame Stiffened Panel

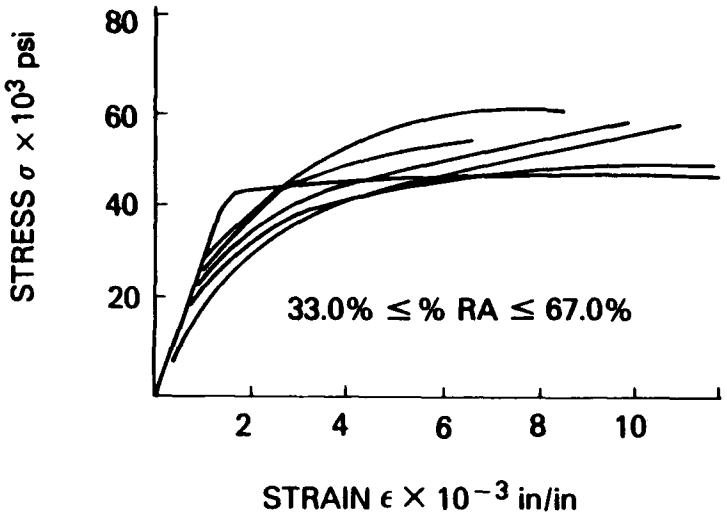

BASE METAL

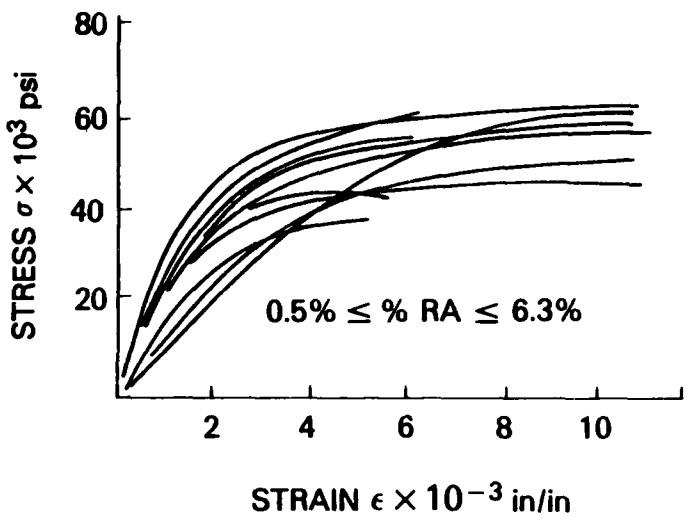

WELD METAL

FIGURE 3: Weld Metal and Base Metal Material Response

BASE METAL

$\sigma_Y = 42.7 \times 10^3$ lb/in^2
$\epsilon_y = 0.00122$ in/in
$\sigma_c = 80.0 \times 10^3$ lb/in^2
$\epsilon_c = 0.680$ in/in
$w_c = 54023.$ lb in/in^3

WELD METAL

$\sigma_y = 49.2 \times 10^3$ lb/in^2
$\epsilon_y = 0.00153$ in/in
$\sigma_c = 63.4 \times 10^3$ lb/in^2
$\epsilon_c = 0.0662$ in/in
$w_c = 4087.$ lb in/in^3

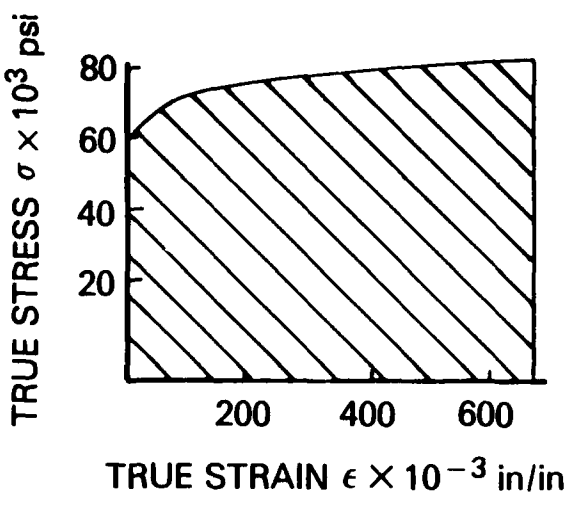

(a) BASE METAL

(HIGH PERCENT REDUCTION OF AREA)

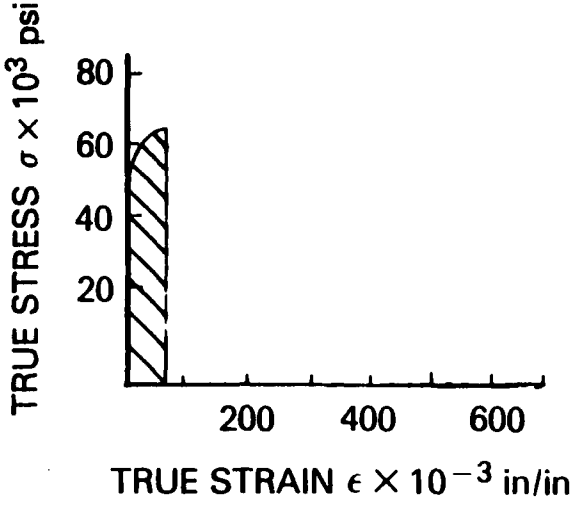

(b) WELD METAL

(LOW PER CENT REDUCTION OF AREA)

FIGURE 4: Weld Metal and Base Metal Cauchy Stress-Logarthmic Strain Response

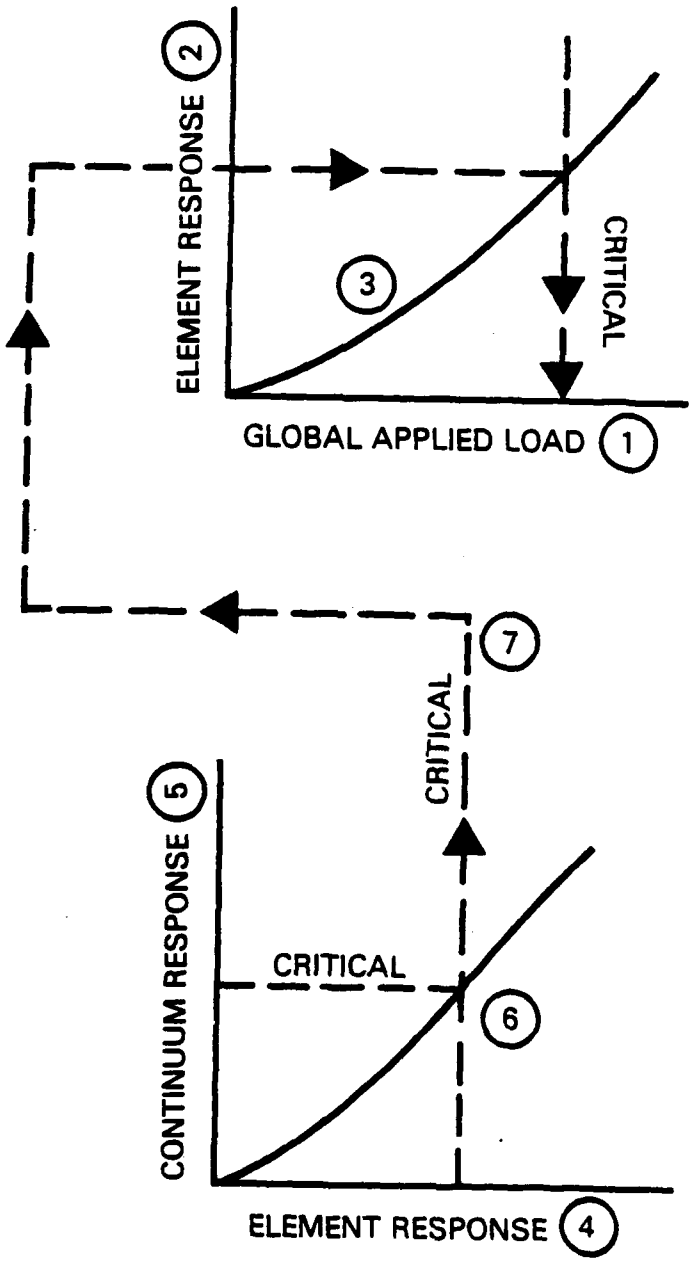

COMPONENT SCALE

1. GLOBAL APPLIED LOAD AS INDEPENDENT VARIABLE
2. ELEMENT RESPONSE AS DEPENDENT VARIABLE
3. ELEMENT RESPONSE VERSUS GLOBAL APPLIED LOAD

DEFECT SCALE

4. ELEMENT RESPONSE AS INDEPENDENT VARIABLE
5. CONTINUUM RESPONSE AS DEPENDENT VARIABLE
6. CONTINUUM RESPONSE VERSUS ELEMENT RESPONSE
7. CRITICAL POINT IN TERMS OF CONTINUUM, ELEMENT AND GLOBAL QUANTITIES

FIGURE 5: Global and Detail Analysis Interaction

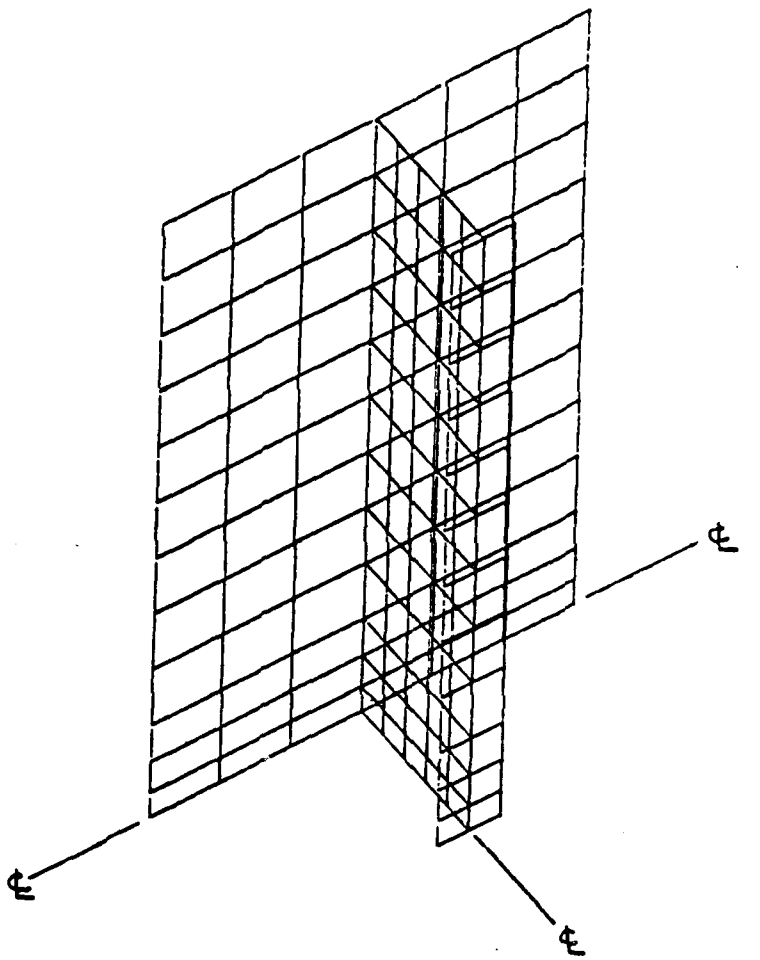

FIGURE 6: Global Response Finite Element Model

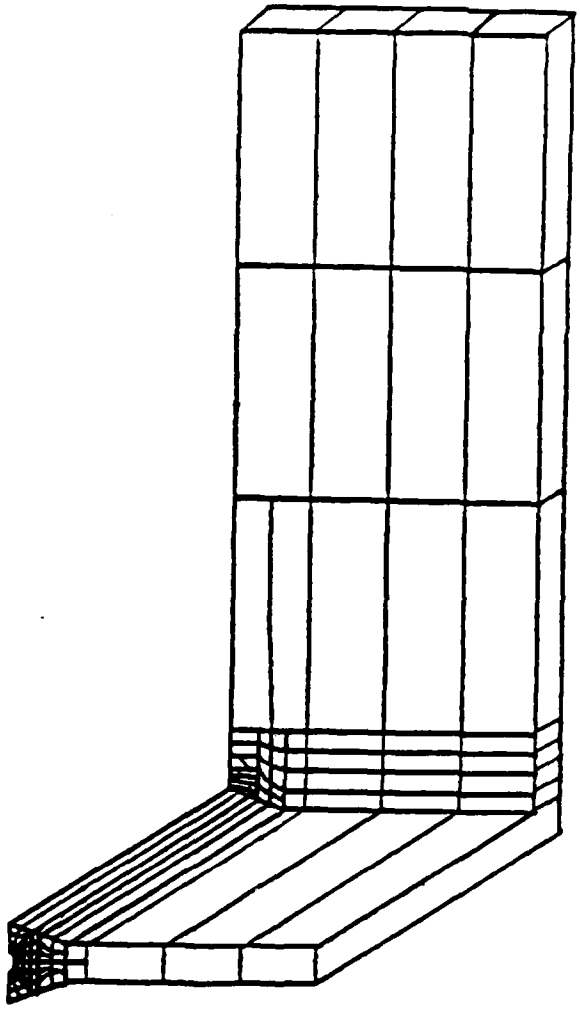

FIGURE 7: Defect Region Detail Finite Element Model

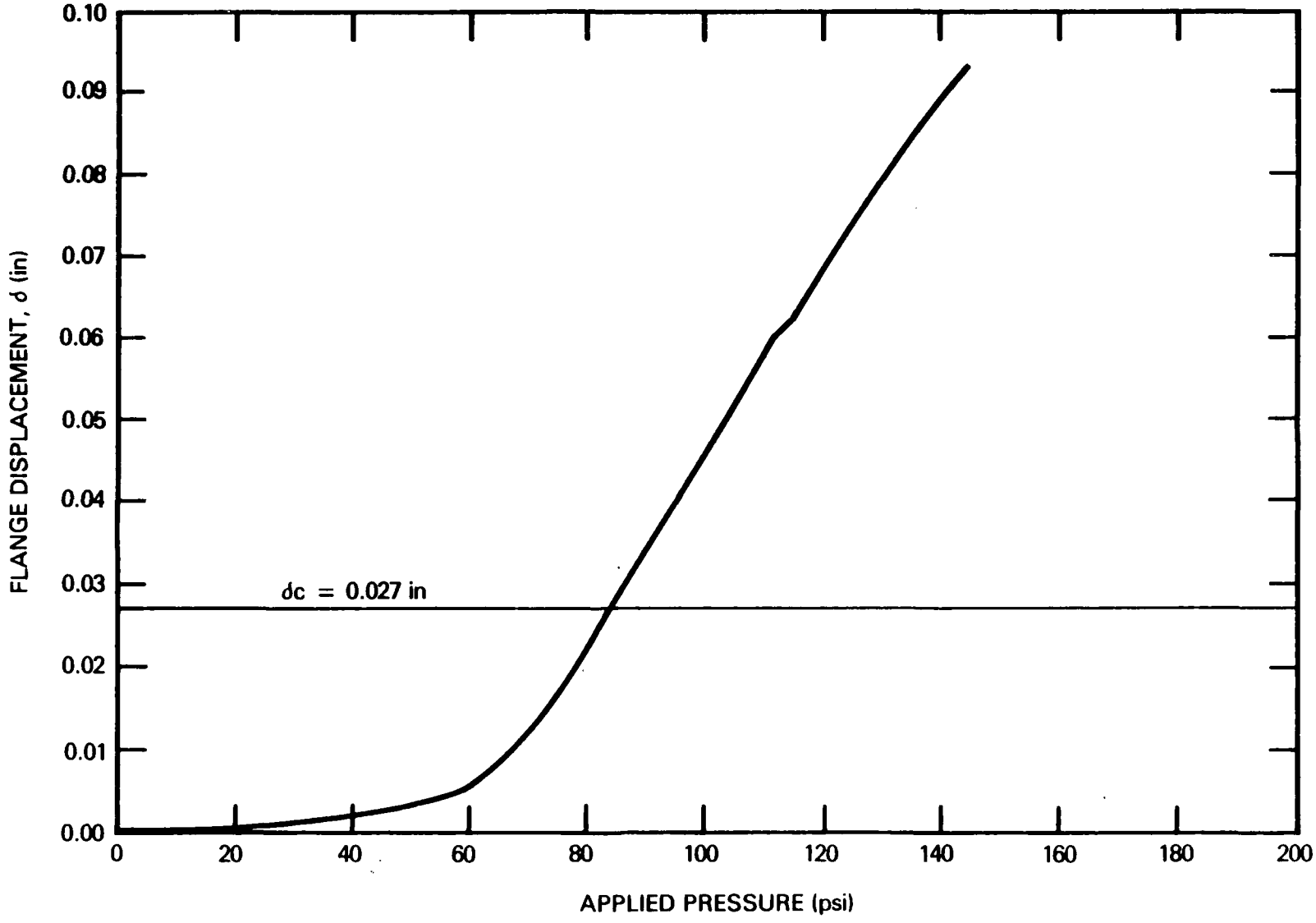

FIGURE 8: Global Load-Displacement Response

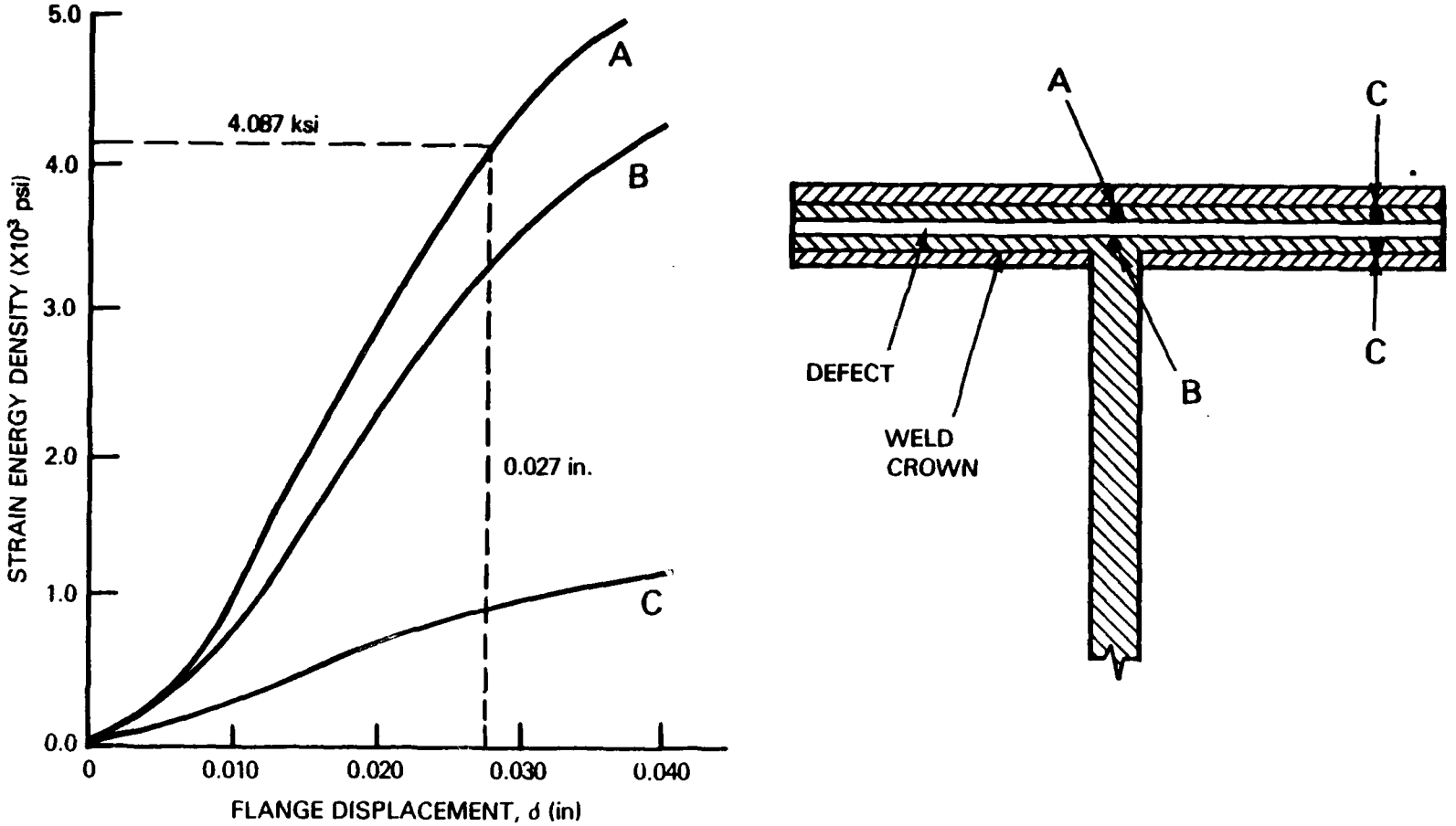

FIGURE 9: Local Strain Energy Density-Displacement Response